An automated framework to quantify exposure of informal urban settlements using UAV and Scan-to-BIM

Mirian Merma[1,2], Christopher Nuñez[1], Carlos Davila[2], Miguel Estrada[2], Marck Regalado[1], Raul Gonzalez[1], Kenny Requelme[1] and Angel Quesquen[2]

[1]Facultad de Ingenieria Civil, Universidad Nacional de Ingenieria, Lima 15333, Peru
[2]GeoGiRD Research Group, Facultad de Ingenieria Civil, Universidad Nacional de Ingenieria, Lima 15333, Peru

mirian.merma.o@uni.pe, christopher.nunez.v@uni.pe, carlos.davila.d@uni.pe, estrada@uni.edu.pe, marck.regalado.e@uni.pe, raul.gonzalez.o@uni.pe, kenny.requelme.c@uni.pe, aquesquenr@uni.pe

Abstract -
Rapid informal urban expansion in high-slope terrains presents a critical challenge for disaster risk management, particularly where foundational digital documentation is absent. This study proposes an automated framework for quantifying urban growth and geodynamic hazard exposure by integrating UAV photogrammetry with a Scan-to-BIM workflow. By processing high-resolution point clouds through noise reduction and normal vector calculation to segment horizontal roof planes, building footprints were extracted and converted into Industry Foundation Classes (IFC) models at a volumetric massing level using IfcOpenShell. Longitudinal analysis revealed a substantial rise in dwelling density across the study periods, with the total built-up area expanding significantly. Critically, spatial intersection with terrain models demonstrated that the most aggressive expansion occurred on the steepest slope categories, highlighting increased population exposure to rockslides according to national risk standards. While the study identifies limitations in detecting irregular geometries and unconventional materials, the proposed framework establishes a reproducible, interoperable BIM–GIS bridge that overcomes the temporal and spatial limitations of traditional monitoring in undocumented urban territories.

Keywords -
Urban Digitalization; UAV Photogrammetry; Scan-to-BIM; Informal Settlements

1 Introduction

The process of urbanization at the global level has experienced rapid growth over the last century. In 1990, only 15% of the urban population lived in urban areas [1]. However, this trend increased significantly during the 20th century. For example, in 2018, more than 58% of the world's population lived in urban areas. Current projections indicate that by 2050, more than approximately 75% of the world's population will live in urban areas [1].

In Peru, given that the formal housing supply has failed to meet demand and due to a lack of urban planning, informal settlements have become the main form of urban growth as massive migration from rural to urban areas [2].

Informal settlements refer to the organization of people in search of housing who occupy vacant lots and take collective action to resolve their urban and social organization problems themselves [3]. In cities such as Lima, the capital of Peru, these settlements have expanded into hillside areas, which are typically by unfavorable geographical conditions and, as a result, are exposed to natural hazards[4].

Currently, multitemporal analysis of urban growth based on remote sensing techniques, including 3D change detection [5], time series analysis of land use [6], and advanced approaches such as multitemporal mergers and segmentation using fuzzy logic [7], has become a high-level tool for monitoring informal urban growth at the regional and metropolitan scale using optical satellite and radar images. However, its application in dense informal contexts has some limitations.

One of the main limitations of using optical satellite images is cloud cover, which affects the acceptance of solar radiation reflected by the surface, reducing the quality of the spectral information available and limiting continuous multitemporal analysis. For example, in Lima, persistent cloud cover for several months of the year makes it difficult to capture clear and consistent images over time [2].

In addition, the construction characteristics of informal settlements may introduce additional challenges. The predominant materials used in housing roofs, such as concrete and dry wood, have spectral signatures similar to those of bare soil, which causes spectral confusion in classification processes and makes it difficult to accurately delimit building footprints. This spectral similarity, combined with high building density and the absence of separation between dwellings on a single block, makes it difficult to delimit building footprints. As a result, urban footprint maps created using spectral signatures have unsatisfactory levels of accuracy [8]. In contexts such as in Lima, characterized by desert conditions and exposed soil surfaces, the spectral similarity between housing roofs and soil is intensified [2], increasing the uncertainty of urban footprint extraction.

Although satellite radar images overcome some limitations associated with cloud cover and dependence on solar radiation, gaps remain in relation to spatial and temporal scale and geometric distortions present in informal urban monitoring [4]. In particular, there is no consensus on the optimal spatial and temporal resolution needed to adequately capture rapid informal urbanization processes [9]. This limitation is evident in studies such as [4], which use Sentinel-1 SAR images to monitor informal growth in areas such as Morro Solar and Lomo de Corvina, where the analysis is based on a set of 14 images acquired between December 2020 and May 2021. This temporal resolution is insufficient to capture rapid changes in real time, while the spatial resolution of 10 m restricts the analysis to estimating occupied areas, without allowing for direct quantification of the number of dwellings.

On the other hand, in informal contexts, the availability of BIM models is practically non-existent, and creating them manually is tedious, costly, and time-consuming [10]. However, generating BIM models from point clouds in these environments can be highly beneficial for gathering information on current conditions, designing interventions, communicating proposals, and raising awareness among residents about environmental issues [11]. Studies such as [12] have shown that the integration of BIM models, visualized on Geographic Information System (GIS)-based platforms, improves the efficiency of urban monitoring and enables applications such as risk assessment in buildings and roads, as well as the development of early warning systems.

In this context, there is a clear need for alternative approaches that allow high-resolution spatial information to be captured with greater temporal flexibility, capable of characterizing the configuration of informal settlements and generating BIM models, particularly those located on slopes exposed to natural hazards.

To address this gap, this study proposes an automated framework for digitizing informal urban environments, integrating data acquired using Unmanned Aerial Vehicle (UAV) with Scan-to-BIM techniques. This approach allows for the automatic extraction of building footprints from point clouds, the generation of BIM models, and the multitemporal quantification of informal housing across different analysis periods. The methodology was applied in hillside areas exposed to rockfalls and landslides, enabling the assessment of informal urban growth and its relationship with the associated hazards, and providing detailed spatial information that can support urban planning and disaster risk management processes. Furthermore, the integration of BIM and GIS provides conceptual support for the representation and analysis of multiscale urban information, aligned with the principles of City Information Modeling and smart cities [13].

2 Related Work

Recent studies have explored the use of data acquired through UAVs and photogrammetric techniques for monitoring informal buildings in urban environments. In [14, 15], the use of oblique photogrammetry with drones was proposed to generate three-dimensional models of the urban environment, allowing the creation of Digital Surface Models (DSM), orthophotographic maps, and 3D models. By analyzing differences between DSMs, they were able to automatically extract and quantitatively analyze informal constructions. Similarly, in [16], a methodology was developed for detecting urban changes by combining differences between dense DSMs and true orthophoto maps (TDOM) generated from aerial images. This approach made it possible to identify changes in both floor plan and height, overcoming the limitations of conventional methods through the use of advanced techniques such as Semi-Global Matching (SGM) and Multi-View Stereo (MVS), and demonstrating high spatial accuracy at the regional scale.

On the other hand, various studies have used synthetic aperture radar (SAR) images and multitemporal approaches for urban growth analysis. In [17], a methodology was presented for the automatic detection of urban changes based on the integration of SAR time series and multispectral data, evaluating the performance of different optical and radar sensors. In the Peruvian context, [2] used SAR images acquired by the Sentinel-1 constellation since 2017 to identify concentrations of urban growth in the Lima metropolitan area, complementing the analysis with high-resolution optical images for the visual identification of informal settlements. Complementarily, in [3], time series of Sentinel-1 SAR images were applied to map the extent of recent occupations in areas with unfavorable soil conditions in the face of seismic events, demonstrating the potential of radar for urban monitoring in vulnerable contexts.

Although these approaches have proven effective for monitoring and detecting informal urban growth, most studies focus on two-dimensional analyses or identifying general patterns of urban expansion. They also have limitations in terms of the precise delimitation and individual quantification of informal dwellings, as well as the automated generation of three-dimensional models that can be integrated into BIM environments, particularly in hillside areas exposed to the risk of rockfalls and landslides.

3 Methodology

Figure 1 illustrates the proposed methodology, which consists of three main components. First, UAV technology is used to efficiently acquire high-resolution data across different analysis periods. These images are processed us-

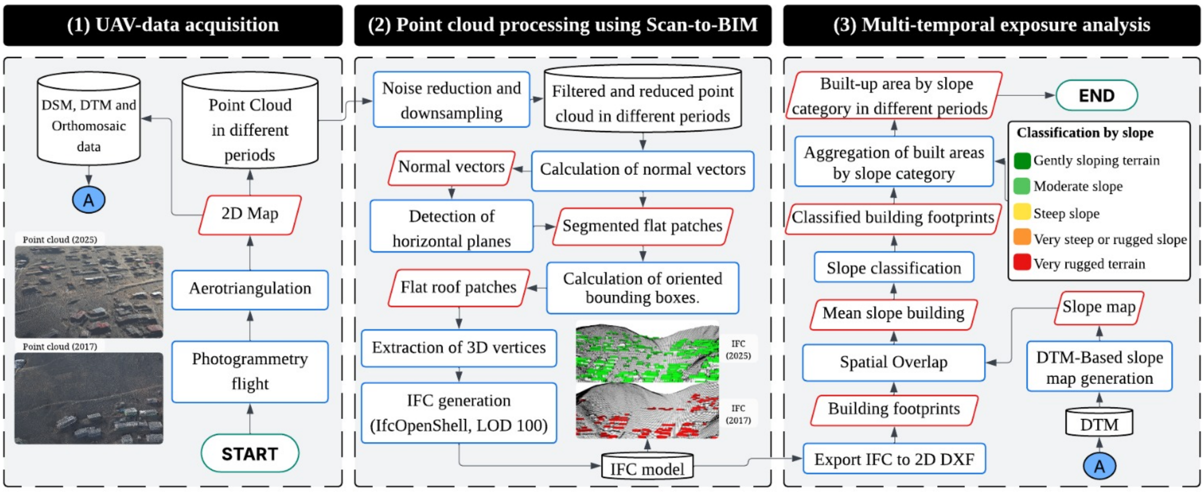

Figure 1. Proposed framework for quantifying exposure in informal urban settlements using UAVs and Scan-to-BIM.

ing photogrammetric techniques to generate point clouds, orthomosaics, and Digital Terrain Models (DTM), which form the geometric and topographic basis of the study.

Second, the generated point clouds are processed using an automated Scan-to-BIM workflow. This process includes noise reduction, normal vector calculation, and the detection of horizontal planes associated with the roofs of the houses. From these geometries, the footprints of the buildings are extracted and BIM models are generated in IFC format using IfcOpenShell, allowing for the digital representation of the houses in the absence of previous documentation.

Finally, the multitemporal analysis is carried out. The IFC models are exported to DXF format to obtain the footprints of the dwellings in a two-dimensional environment, which are intersected with slope maps derived from the DTM. Each footprint is assigned an average slope value, which is then classified into the five ranges of slope established by the National Center for Disaster Risk Estimation, Prevention and Reduction (CENEPRED) of Peru. The aggregation of areas by slope level for each period allows for a temporal comparison of urban occupation based on its exposure. This classification characterizes the terrain's susceptibility to geodynamic hazards, such as rockslides [4] . Finally, the aggregation of residential areas by slope level for each analysis period allows for a temporal comparison of urban occupation, assessing its exposure to hazards associated with highly susceptible terrain.

3.1 Study area

The district of Comas (Figure 2b), located in the province of Lima (Figure 2a), department of Lima, Peru, covers a total area of 48.75 km2 and has 14 zones and 32 urbanizations, with a population density of 9,989.3 inhabitants per square kilometer [18] (see Fig. 2). This study focuses on the Año Nuevo settlement, Zone A (Figure 2c), and covers an area of approximately 0.7 km² [4].

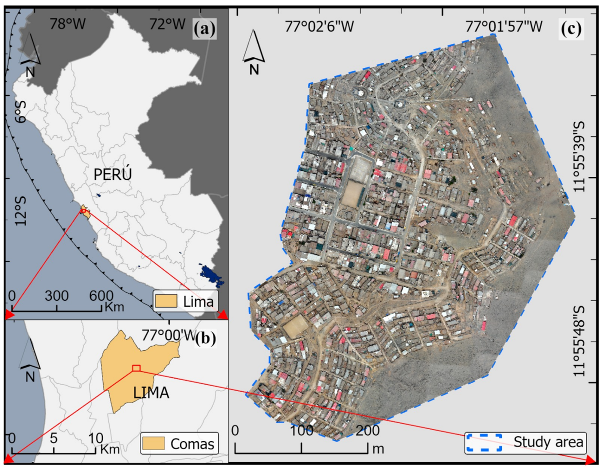

Figure 2. Location map of the study area.

3.2 UAV data acquisition

Data acquisition for the generation of point clouds and 2D maps was performed using photogrammetry for the periods of 2017 and 2025. The flight parameters are presented in Table 1, which summarizes the specifications of the UAV flights implemented.

Table 1. Technical specifications of UAV flights.

Data	2017 Flight	2025 Flight (%)
UAV model	DJI Phantom 3	DJI Mavic 3 Enterprise (M3E)
Sensor	Integrated RGB camera, FC300X model	High-resolution integrated RGB camera
Camera resolution	12 MP (4000 × 3000 px)	20 MP (5280 × 3956 px)
GSD	7.7 cm/pixel	4.5 cm/pixel

3.3 Scan-to-BIM workflow

The photogrammetric data was processed using DJI Terra 5.1.1, from which the main photogrammetric products were generated, including the DSM, DTM, orthomosaic, and the dense point cloud. Based on the generated point cloud, the Scan-to-BIM methodology was used to produce as-built BIM models of existing buildings, enabling digital documentation and geometric representation of the built environment in areas where no previous BIM information existed [19, 20].

3.3.1 Point cloud preprocessing

The raw datasets for 2017 and 2025 were subjected to noise reduction and spatial downsampling at a 0.05 m resolution. This resolution was selected as a compromise between computational efficiency and the preservation of geometric features relevant for roof segmentation, as finer resolutions did not significantly improve segmentation results while substantially increasing processing cost. This preprocessing balanced computational efficiency with geometric fidelity, significantly reducing the point density while preserving the structural features necessary for morphological analysis (see Tab. 2).

Table 2. Point cloud preprocessing parameters for the 2017 and 2025 datasets.

Dataset	Raw Points	Processed Points	Reduction (%)
2017	30,313,508	11,413,767	62.3%
2025	41,380,614	11,170,087	73.0%

3.3.2 Automated roof detection and segmentation

Roof surfaces were identified by detecting horizontal planes within the processed point clouds. Using the Open3D library, surface normals were estimated via KD-tree–based nearest-neighbor searches. Planar patches were segmented using the Oriented Bounding Box (OBB) method, supported by covariance analysis and local density criteria.

This simplification was guided by the study area, where roofs are predominantly flat or near-horizontal, making them the most reliable feature for building detection. While effective in this context, it may limit applicability in areas with more complex roof geometries. This process identified 1,659 horizontal planes for the 2017 dataset and 1,908 for 2025, forming the geometric basis for the building models.

3.3.3 Semantic alignment and interoperability strategy

The segmented point cloud data were transformed into a structured digital environment by extracting the 3D vertices of detected roof planes to define individual building contours. These geometries were converted into parametric BIM entities at LOD 100, representing the general volumetric massing of the dwellings. The reconstruction process was automated using IfcOpenShell, enabling a reproducible workflow for the generation of longitudinal models for 2017 and 2025.

The workflow was designed to comply with the FAIR principles for geospatial data [21] and to support BIM–GIS integration. The use of IFC as a native data structure enables direct integration with IfcOpenShell for geometry generation, attribute handling, and standardized data exchange, ensuring reproducibility and compatibility with established BIM processing tools [22, 23]. Although each dwelling corresponds conceptually to a single building, the geometry was instantiated as IfcSpace entities as a pragmatic modeling simplification within the implemented workflow. We acknowledge that this choice does not comply with IFC spatial hierarchy conventions, and that each entity should be assigned to an IfcBuilding according to IFC 4.3.

To reduce reprojection errors and information loss during IFC–CityGML transformations, global georeferencing was embedded directly within the IFC output [23]. By adopting LOD 100, the methodology supports efficient processing of high-density informal settlements while enabling standardized and interoperable BIM model generation despite irregular urban morphologies [24, 25].

This approach demonstrates that the absence of prior documentation or the irregular morphology of the built environment does not preclude the creation of standardized, interoperable BIM models [26].

3.3.4 Multitemporal Analysis

Multitemporal analysis was performed to evaluate the evolution of urban occupation in hillside areas between 2017 and 2025, based on the relationship between built-up areas and terrain slope. The main input used was the footprints of the dwellings extracted from the IFC models generated using the Scan-to-BIM methodology, which made it possible to represent urban occupation in a homogeneous environment for both periods.

The footprints of the buildings were integrated with slope maps obtained from the digital terrain model (DTM), allowing each built unit to be assigned a representative average slope value using zonal statistical methods. These values were then classified into the five slope levels established by CENEPRED. Finally, the built-up areas were aggregated by slope level for each period of analysis, enabling a temporal comparison of urban growth based on the topographical conditions of the terrain.

3.3.5 Quantitative Accuracy Evaluation

Numerical validation was performed by comparing the extracted features with a manual ground truth using pixel-by-pixel confusion matrices. The 2025 results show solid performance (precision: 0.919; F1 score: 0.703), thanks to the high resolution and precision of the DJI Mavic 3 drone camera, which minimizes noise. In 2017, although precision was 0.900, the F1 score dropped to 0.384. This lower precision is attributed to a more dispersed and noisy point cloud, resulting from lower-resolution sensors and a higher flight altitude, which, combined with unconventional surface materials, increased false negatives. This evaluation quantifies the reliability and limitations of the proposed automation system in the face of variations in the density and accuracy of the source data.

Table 3. Performance metrics for automated building footprint extraction.

Year	Raw Accuracy	Precision Points	Recall	F1 Score (%)
2017	0.9	0.432	0.345	38.4
2025	0.919	0.578	0.896	70.3

4 Results and discussions

The Scan-to-BIM workflow successfully transformed spatial point cloud data into georeferenced, interoperable BIM models in IFC format. By extracting building footprints and altitudes from detected horizontal planes (roofs), volumetric representations of the informal settlement were generated for the years 2017 and 2025.

4.1 Longitudinal modeling analysis

The automated reconstruction process identified a clear increase in the number of reconstructed dwellings over the eight-year study period.

- 2017 Dataset: Around 1000 dwellings were reconstructed as parametric IfcSpace entities, representing the spatial distribution and volumetric configuration of the settlement at the baseline year (Fig. 3).
- 2025 Dataset: Using identical reconstruction parameters, almost 1600 dwellings were generated. This corresponds to an increase of 682 dwellings, or around 60%, relative to 2017, providing a quantitative indicator of built-up expansion and informal growth within the study area (Fig. 4).

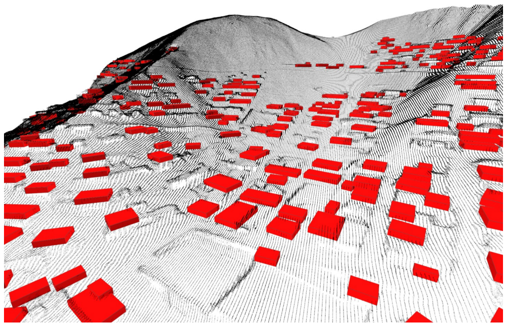

Figure 3. Reconstructed dwelling distribution for the 2017 dataset.

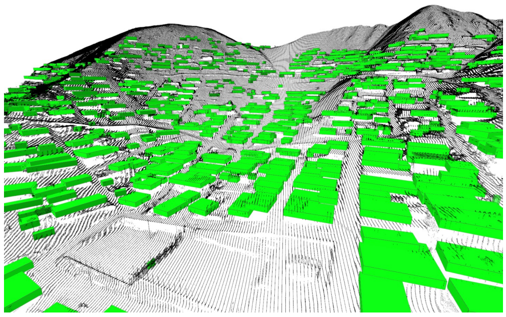

Figure 4. Reconstructed dwelling distribution for the 2025 dataset.

4.2 Multitemporal analysis

The multitemporal analysis made it possible to generate thematic maps of urban occupation for the years 2017 and 2025, as shown in Figures 5 and 6, which represent the footprints of buildings within the study area, each footprint associated with an average slope value and classified into five levels according to the ranges established by

CENEPRED, which allowed for the spatial visualization of the area where the dwellings are located in relation to the topographical conditions of the terrain.

In addition, summary tables were prepared that quantify the total area occupied by dwellings for each slope level and for each analysis period, as shown in table 4. These results made it possible to compare urban occupation between the two years, revealing differences in the spatial distribution of built-up areas according to slope level.

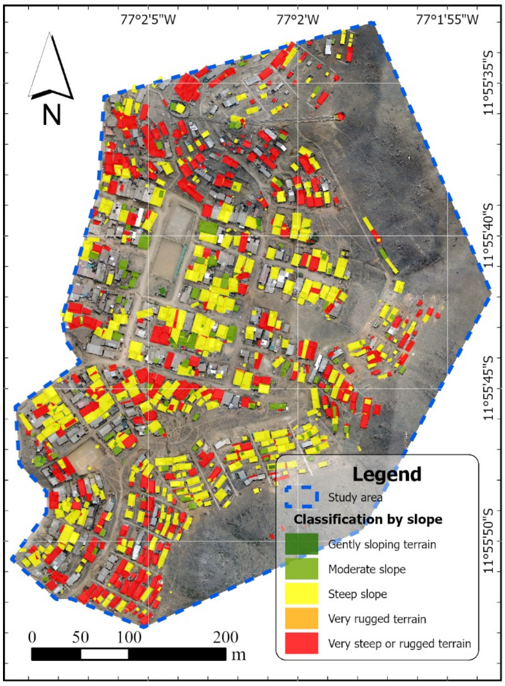

Figure 5. Map of building footprints in 2017 classified by terrain slope levels.

Table 4. Distribution of built-up area by terrain slope level, 2017 and 2025.

Classification by slope	Slope	Area 2017 (m^2)	Area 2025 (m^2)
	< 5º	173,75	416,25
	5º - 15º	4.005,75	6.287,25
	15º - 25º	21.737,25	21.813,75
	25º - 45º	76,25	924,75
	> 45º	18.766,75	33.142,75
Total area (m^2)		44.759,75	62.584,75

5 Conclusions

This study proposes an automated framework for quantifying the exposure of informal urban settlements over different time periods using UAVs and Scan-to-BIM. The results suggest that the proposed approach allows for: (1) automated digitization of building footprints, (2) generation of BIM models in LOD 100 and their export in IFC format, and (3) multitemporal analysis of urban growth and exposure to hazards. In this sense, the methodology reduces some of the limitations associated with the spatial and temporal resolution of traditional satellite image-based approaches, by providing high-resolution spatial data with greater temporal flexibility. It also minimizes the need for manual and repetitive processing of point cloud data and geospatial analysis.

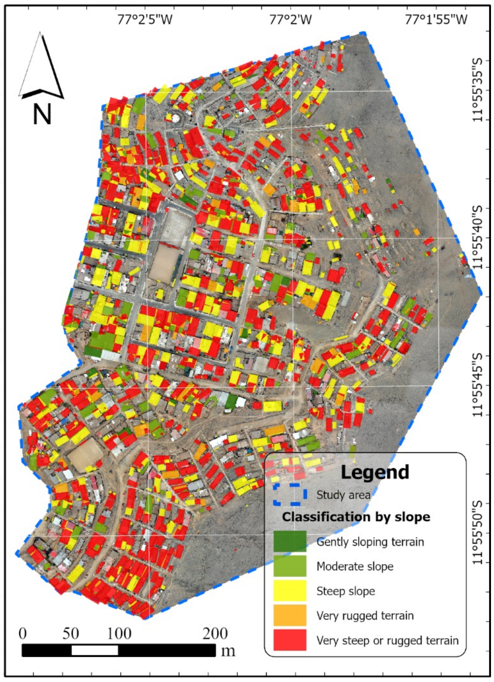

Figure 6. Map of building footprints in 2025 classified by terrain slope levels.

Despite these advantages, the study also highlights limitations related to the accurate detection of informal dwellings, especially in cases where roof geometries are not flat or are irregular. The presence of unconventional roofing materials, such as corrugated iron and wood, as well as the lack of minimum separation between dwellings, affected the correct delimitation of building footprints. In addition, high noise levels in the point cloud led to the misclassification of surfaces that do not correspond to dwellings, which influenced the accuracy of urban occupation estimates. In this context, it is suggested that future research incorporate automated tools for the detection of non-flat surfaces, as well as methods for automatic classification and noise reduction in the point cloud.

References

[1] Naledzani Mudau and Paidamwoyo Mhangara. Mapping and assessment of housing informality using object-based image analysis: A review. *Urban Science*, 7(3), 2023. ISSN 2413-8851. doi:10.3390/urbansci7030098. URL https://www.mdpi.com/2413-8851/7/3/98.

[2] Luis Moya, Marta Vilela, Javier Jaimes, Briggite Espinoza, Jose Pajuelo, Nicola Tarque, Sandra Santa-Cruz, Pablo Vega-Centeno, and Fumio Yamazaki. Vulnerabilities and exposure of recent informal urban areas in lima, peru. *Progress in Disaster Science*, 23:100345, 2024. ISSN 2590-0617. doi:https://doi.org/10.1016/j.pdisas.2024.100345. URL https://www.sciencedirect.com/science/article/pii/S2590061724000358.

[3] L. Moya, F. Garcia, C. Gonzales, M. Diaz, C. Zavala, M. Estrada, F. Yamazaki, S. Koshimura, E. Mas, and B. Adriano. Brief communication: Radar images for monitoring informal urban settlements in vulnerable zones in lima, peru. *Natural Hazards and Earth System Sciences*, 22(1):65–70, 2022. doi:10.5194/nhess-22-65-2022. URL https://nhess.copernicus.org/articles/22/65/2022/.

[4] Frank Angel Mallma Acuña. Herramientas geomáticas para la evaluación de zonas urbanas amenazadas por deslizamiento de material en laderas, 2019. URL https://hdl.handle.net/20.500.14138/2005.

[5] Wen Xiao, Hui Cao, Miao Tang, Zhenchao Zhang, and Nengcheng Chen. 3d urban object change detection from aerial and terrestrial point clouds: A review. *International Journal of Applied Earth Observation and Geoinformation*, 118:103258, 2023. ISSN 1569-8432. doi:https://doi.org/10.1016/j.jag.2023.103258. URL https://www.sciencedirect.com/science/article/pii/S1569843223000808.

[6] Peng Dou and Zhen Han. Quantifying land use/land cover change and urban expansion in dongguan, china, from 1987 to 2020. *IEEE Journal of Selected Topics in Applied Earth Observations and Remote Sensing*, 15:201–209, 2022. doi:10.1109/JSTARS.2021.3133703.

[7] Ahmed Alejandro Cardona-Mesa, Rubén Darío Vásquez-Salazar, Juan Camilo Parra, César Olmos-Severiche, Carlos M. Travieso-González, and Luis Gómez. A methodology for the multitemporal analysis of land cover changes and urban expansion using synthetic aperture radar (sar) imagery: A case study of the aburrá valley in colombia. *Remote Sensing*, 17(3), 2025. ISSN 2072-4292. doi:10.3390/rs17030554. URL https://www.mdpi.com/2072-4292/17/3/554.

[8] Gonzalo Rodolfo Peña Zamalloa, Yumin Tan, and Lingfeng He. Modelling human settlement growth and fringe patterns in the andes through remote sensing and deep learning. *Cities*, 170:106660, 2026. ISSN 0264-2751. doi:https://doi.org/10.1016/j.cities.2025.106660. URL https://www.sciencedirect.com/science/article/pii/S0264275125009631.

[9] Gundegmaa Chinzorig, Md. Omar Sarif, and Ayyoob Sharifi. An analysis of the effectiveness of urban master plans in controlling and regulating urban growth in ulaanbaatar, mongolia. *Cities*, 170:106713, 2026. ISSN 0264-2751. doi:https://doi.org/10.1016/j.cities.2025.106713. URL https://www.sciencedirect.com/science/article/pii/S0264275125010169.

[10] T. Zhou, L. Lv, J. Liu, and J. Wan. Application of uav oblique photography in real scene 3d modeling. *The International Archives of the Photogrammetry, Remote Sensing and Spatial Information Sciences*, XLIII-B2-2021:413–418, 2021. doi:10.5194/isprs-archives-XLIII-B2-2021-413-2021. URL https://isprs-archives.copernicus.org/articles/XLIII-B2-2021/413/2021/.

[11] Victoria Rautenbach, Yvette Bevis, Serena Coetzee, and Carin Combrinck. Evaluating procedural modelling for 3d models of informal settlements in urban design activities. *South African Journal of Science*, 111(11/12):10, Nov. 2015. doi:10.17159/sajs.2015/20150100. URL https://sajs.co.za/article/view/3804.

[12] C.-H. Yang, C. Stemmler, N. Wolf, M. Koppe, T. Rudolph, and A. Müterthies. Fusion of bim and sar for innovative monitoring of urban movement – towards 4d digital twin. *The International Archives of the Photogrammetry, Remote Sensing and Spatial Information Sciences*, XLVIII-G-2025:1627–1632, 2025. doi:10.5194/isprs-archives-XLVIII-G-2025-1627-2025. URL https://isprs-archives.copernicus.org/articles/XLVIII-G-2025/1627/2025/.

[13] Jianyong Shi, Zeyu Pan, Liu Jiang, and Xiaohui Zhai. An ontology-based methodology to establish city information model of digital twin city by

merging bim, gis and iot. *Advanced Engineering Informatics*, 57:102114, 2023. ISSN 1474-0346. doi:https://doi.org/10.1016/j.aei.2023.102114. URL https://www.sciencedirect.com/science/article/pii/S1474034623002422.

[14] T. Zhou, L. Lv, J. Liu, and J. Wan. Application of uav oblique photography in real scene 3d modeling. *The International Archives of the Photogrammetry, Remote Sensing and Spatial Information Sciences*, XLIII-B2-2021:413–418, 2021. doi:10.5194/isprs-archives-XLIII-B2-2021-413-2021. URL https://isprs-archives.copernicus.org/articles/XLIII-B2-2021/413/2021/.

[15] Carlos Davila, Angel Quesquen, Fernando Garcia, Brigitte Puchoc, Oscar Solis, Julian Palacios, Jorge Morales, and Miguel Estrada. Assessment of building vulnerability to tsunami in ancon bay, peru, using high-resolution unmanned aerial vehicle imagery and numerical simulation. *Drones*, 9(6), 2025. ISSN 2504-446X. doi:10.3390/drones9060402. URL https://www.mdpi.com/2504-446X/9/6/402.

[16] David Marzi, Erith Munoz Rios, Antonietta Sorriso, Fabio Dell'Acqua, and Paolo Gamba. Joint multitemporal sar and optical mapping of urban changes. *International Journal of Microwave and Wireless Technologies*, 16(3):359–370, 2024. doi:10.1017/S175907872400031X.

[17] X. Zhu, G. Pang, P. Chen, Y. Tao, Y. Zhang, and X. Zuo. Research on urban construction land change detection method based on dense dsm and tdom of aerial images. *The International Archives of the Photogrammetry, Remote Sensing and Spatial Information Sciences*, XLII-3/W10:205–210, 2020. doi:10.5194/isprs-archives-XLII-3-W10-205-2020. URL https://isprs-archives.copernicus.org/articles/XLII-3-W10/205/2020/.

[18] Municipalidad de Comas. Geografía, s. f. URL https://www.municomas.gob.pe/distrito/geografia. Consultado el 16 de enero de 2026.

[19] Sebastian Ochmann, Richard Vock, and Reinhard Klein. Automatic reconstruction of fully volumetric 3d building models from oriented point clouds. *ISPRS Journal of Photogrammetry and Remote Sensing*, 151:251–262, 2019. ISSN 0924-2716. doi:https://doi.org/10.1016/j.isprsjprs.2019.03.017. URL https://www.sciencedirect.com/science/article/pii/S0924271619300863.

[20] Chao Wang, Yong K. Cho, and Changwan Kim. Automatic bim component extraction from point clouds of existing buildings for sustainability applications. *Automation in Construction*, 56:1–13, 2015. ISSN 0926-5805. doi:https://doi.org/10.1016/j.autcon.2015.04.001. URL https://www.sciencedirect.com/science/article/pii/S0926580515000734.

[21] Linda van den Brink. *Geospatial Data on the Web*. Dissertation (tu delft), Delft University of Technology, 2018.

[22] Ying Liang and Yi Tan. A systematic literature review of ifc-to-citygml conversion. In Dezhi Li, Patrick X. W. Zou, Jingfeng Yuan, Qian Wang, and Yi Peng, editors, *Proceedings of the 28th International Symposium on Advancement of Construction Management and Real Estate*, pages 1265–1278, Singapore, 2024. Springer Nature Singapore. ISBN 978-981-97-1949-5.

[23] Mohammed Sani and Alias Rahman. Gis and bim integration at data level: A review. *ISPRS - International Archives of the Photogrammetry, Remote Sensing and Spatial Information Sciences*, XLII-4/W9: 299–306, 10 2018. doi:10.5194/isprs-archives-XLII-4-W9-299-2018.

[24] F. Bianconi, M. Filippucci, F. Cornacchini, and A. Migliosi. The impact of google's apis on landscape virtual representation. *The International Archives of the Photogrammetry, Remote Sensing and Spatial Information Sciences*, XLVIII-4/W9-2024:91–98, 2024. doi:10.5194/isprs-archives-XLVIII-4-W9-2024-91-2024. URL https://isprs-archives.copernicus.org/articles/XLVIII-4-W9-2024/91/2024/.

[25] Edoardo De Santis and Pieter Pauwels. Actor-based framework for interoperable bim data management. In *Proceedings of the 2025 European Conference on Computing in Construction*, volume 6 of *Computing in Construction*, Porto, Portugal, July 2025. European Council on Computing in Construction. ISBN 978-9-083451-31-2. doi:10.35490/EC3.2025.314. URL https://ec-3.org/publications/conference/paper/?id=EC32025_314.

[26] Nuno Abreu, Andry Pinto, Aníbal Matos, and Miguel Pires. Procedural point cloud modelling in scan-to-bim and scan-vs-bim applications: A review. *ISPRS International Journal of Geo-Information*, 12(7), 2023. ISSN 2220-9964. doi:10.3390/ijgi12070260. URL https://www.mdpi.com/2220-9964/12/7/260.